



106
185
THS



3 1293 00701 4008

LIBRARY
Michigan State
University

This is to certify that the

thesis entitled

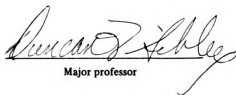
KINETIC EQUATIONS FOR THE PRECIPITATION OF CARBONATES
WITHIN THE THERMODYNAMIC STABILITY FIELD OF DOLOMITE

presented by

Robert E. Dedoes

has been accepted towards fulfillment
of the requirements for

Master of Science degree in Geological Sciences


Major professor

Date May 18, 1987



RETURNING MATERIALS:

Place in book drop to
remove this checkout from
your record. FINES will
be charged if book is
returned after the date
stamped below.

JAN 05 1963

027

KINETIC EQUATIONS FOR THE PRECIPITATION OF CARBONATES
WITHIN THE THERMODYNAMIC STABILITY FIELD OF DOLOMITE

By

Robert E. Dedoes

A THESIS

Submitted to
Michigan State University
in partial fulfillment of the requirements
for the degree of

MASTER OF SCIENCE

Department of Geological Sciences

1987

Copyright by

ROBERT E. DEDOES

1987

4566117

ABSTRACT

KINETIC EQUATIONS FOR THE PRECIPITATION OF CARBONATES WITHIN THE THERMODYNAMIC STABILITY FIELD OF DOLOMITE

By

Robert E. Dedoes

Equations which can potentially describe the precipitation of carbonate phases within the thermodynamic stability field of dolomite are derived. The equations are applicable only when all precipitating phases are nucleating onto the same finite number of nucleation sites. The equations appear consistent with published experimental data concerning the precipitation of carbonates within the thermodynamic stability field of dolomite. The equations allow several phases to compete with each other for the same nucleation sites and by doing such, they account for both Ostwald's step rule occurring during carbonate substrate to dolomite transformations and for the distribution of carbonates in marine waters. The equations also suggest that the number of nucleation sites per unit volume of material being transformed is an important variable in the rate of transformation of carbonate sediments to dolomite. The equations can also be potentially used to predict porosity in dolomitic rocks.

TABLE OF CONTENTS

LIST OF TABLES	ii
LIST OF FIGURES	iii
I INTRODUCTION	1
II DERIVATION OF THE EQUATIONS	2
A. Time-dependent heterogeneous nucleation and time-independent growth	9
B. Time-independent heterogeneous nucleation and time-dependent growth	11
III THE VALIDITY OF THE DERIVED EQUATIONS AS COMPARED TO EXPERIMENTS	11
IV APPLICATION OF THE EQUATIONS TO EXPERIMENTAL AND NATURAL SITUATIONS	
A. Proposed explanation for sequences of metastable phases prior to the precipitation of the stable phases (Ostwald's steps)	15
B. Proposed explanation for the distribution of carbonates from marine-type waters	19
C. Proposed explanation for the effect of substrate grain size on the transformation rate	22
D. Proposed equation describing the porosity and permeability of dolomitic rocks	23
V CONCLUSION	24
APPENDIX	
A. Experimental procedure	25
B. Results	26
C. Interpretation of results	26
REFERENCES	33

LIST OF TABLES

Table 1:	EXPERIMENTAL RESULTS FROM X-RAY DIFFRACTION	27
Table 2:	DISTRIBUTION OF MARINE CARBONATES	20

LIST OF FIGURES

Figure 1: Reaction progress versus time curves	8
Figure 2: Calcite to dolomite transformation	12
Figure 3: Nucleation rate per site versus supersaturation	16
Figure 4: Proposed curves for coarse and fine material	23

I INTRODUCTION

Numerous studies have been concerned with the precipitation of dolomite from aqueous solutions onto substrates under natural conditions (see Fairbridge 1957, Ingerson 1962, Friedman and Sanders 1967, Zenger 1972, Zenger and Dunham 1980, Morrow 1982a and 1982b). Two conclusions can be drawn from the current studies of dolomite precipitation under natural conditions. First, dolomite occurs in many different types of geologic environments yet it is absent from many others where it is thermodynamically stable. Second, many types of metastable carbonate phases precipitate within the thermodynamic stability field of dolomite. These two conclusions indicate that dolomite can precipitate under earth surface conditions and there is a kinetic control of the precipitation of carbonates within the thermodynamic stability field of dolomite.

Several experimental investigations have been undertaken to identify the kinetic control(s) of carbonate precipitation within the thermodynamic stability field of dolomite. Katz and Matthews (1977) found that the dissolution-reprecipitation transformation of aragonite and calcite to dolomite occurred via a sequence of metastable carbonate phases (Ostwald's step rule). Baker and Kastner (1981) found that sulfate inhibits the transformation of calcite to dolomite. Gaines (1980) found that in an aqueous solution both magnesium calcite and aragonite underwent a faster transformation to dolomite than did low magnesium calcite. He also found that the Mg/Ca ratio, the addition of dolomite crystals, and the addition of certain additives all influence the transformation of aragonite to calcite.

Kinetic processes of crystallization cannot be

directly interpreted from experimental results without the aid of theoretical kinetic equations. Currently there have been no studies that investigate the theoretical aspects of the kinetics of precipitation of carbonate phases within the thermodynamic stability field of dolomite. The purpose of this study is to develop basic theoretical kinetic equations for dolomite precipitation. The results of this study are the derivation of equations which describe the simultaneous precipitation of several crystalline phases from solution onto a substrate. These equations are an extension of the works of Johnson and Mehl (1939) and Avrami (1939, 1940, 1941) to multiphase systems. The study also shows how the equations can be used to interpret existing data on carbonate precipitation within the thermodynamic stability field of dolomite.

II DERIVATION OF THE EQUATIONS

The kinetic equations for the precipitation of carbonates within the thermodynamic stability field of dolomite are based on two kinetic processes of precipitation: nucleation and the growth of crystals from those nuclei. It will be assumed that nucleation of carbonates within the thermodynamic stability field of dolomite occurs only on a finite number of nucleation sites and that all precipitating phases can nucleate on the same nucleation sites. The general derivation of the equations is based on the works of Johnson and Mehl (1939) and Avrami (1939, 1940, 1941).

Consider a volume of carbonate sediments bathed by an aqueous solution whose volume is uV . The volume remains as uV until a time $t=\tau$ when the first nucleus of a transforming carbonate phase nucleates somewhere in uV .

During the time interval $\tau + d\tau$ the change in the number of nuclei is given by:

$$dN = {}^uV {}^vI d\tau \quad (1)$$

where vI is the nucleation rate for one type of nucleation site per unit volume. A single type of nucleation site is any place or places on a substrate where the ΔG of nucleation for a phase is the same for that phase. Nucleation sites can be defects, corners, kinks, etc. on a substrate. ${}^T V$ is the volume of uV left after the precipitation of nuclei during the interval $\tau + d\tau$. It will be assumed to be equal to uV .

The number of nuclei formed at any time since the onset of nucleation is found by integrating Equation (1) as follows:

$$N(t) = {}^uV \int_{\tau=0}^{\tau=t} {}^vI d\tau \quad (2)$$

Assuming that the nucleus of a carbonate phase grows such that G_{tx} , G_{ty} , G_{tz} are the growth vectors along the x, y, and z axes respectively, then the amount of growth per unit time for three dimensions is $G_{tx} dt \times G_{ty} dt \times G_{tz} dz = R(G_t dt)^3$; for two dimensional growth, $G_{tx} dt \times G_{ty} dt = R(G_t dt)^2$; for one dimensional growth, $G_{tx} dt = R(G_t dt)$ and the general form for any dimensional growth is $R(G_t dt)^n$ where R is a geometric shape factor. The small t in G_t indicates that the growth vector G can vary in magnitude with time.

The instantaneous change in volume of a growing crystal is given by:

$$dV = R(G_{(t)}dt)^n \quad (3)$$

The volume change for a single crystal since the onset of nucleation is:

$$V(t) = R \int_{t=\tau}^t (G_{(t)}dt)^n \quad (4)$$

The total volume change since the onset of nucleation of the carbonate phase is the product of Equations (2) and (4):

$$A_{V(t)} = u_V \int_{\tau=0}^t v_I \left[R \int_{t=\tau}^t (G_{(t)}dt)^n \right] d\tau \quad (5)$$

Consider many phases precipitating into the same nucleation sites. Each phase will have a volume at time t given by Equation (5). The total volume at time t since the onset of nucleation for all phases is:

$$V(t)^{\text{total}} = A_{V(t)} + B_{V(t)} + \dots + N_{V(t)} \quad (6)$$

where $A_{V(t)}$, $B_{V(t)}$, \dots , $N_{V(t)}$ are the volumes at time t since the onset of nucleation of phases A, B, \dots , N.

Substituting the $V(t)$ for each phase as given in Equation (5) into Equation (6) gives:

$$V^{\text{total}} = u_V \left[\sum_{i=A}^N \int_{\tau=0}^t v_I \left[R \int_{t=\tau}^t (G_{(t)}dt)^n \right] d\tau \right] \quad (7)$$

Up to this point, the covering up of nucleation sites by growing

crystals and the mutual interference of growing crystals has not been considered. These two processes are important in most precipitation systems and therefore should be considered. This will be done using the treatment of Avrami (1939, 1940). This treatment is valid only under the following conditions: nucleation occurs randomly throughout the volume, and impinging crystals meet with a common interface, but no growth occurs along this interface.

To mathematically describe the covering up of nucleation sites by growing crystals and the mutual interference of growing crystals, an extended volume must first be defined. The extended volume is the volume of material which could have nucleated and grown if there was no interference by crystals during growth and no covering up of nucleation sites by crystals during their growth. In an extended volume, nucleation is occurring within crystals as well as between them. The growth of the crystals is in free space and unimpeded through each other.

In the extended volume, during the interval $\tau + d\tau$, there are $v_I^u V d\tau$ nuclei formed in the open nucleation sites of one type and $v_I^T V d\tau$ nuclei formed in the nucleation sites of that type now covered up by crystals. The change in the number of nuclei since the onset of nucleation is given by:

$$dN = v_I (T_V + u_V) d\tau \quad (8)$$

where T_V and u_V are the volumes of the transformed and untransformed regions respectively.

The number of nuclei formed during a time interval since the onset of nucleation is:

$$N = u_V \int_{\tau=0}^t v_I d\tau \quad (9)$$

T_V is negligible for the small instance $\tau + d\tau$ thus $u_V + T_V = u_V$.

Multiplying Equations (9) and (4) gives the extended volume of carbonate phases precipitated since the onset of nucleation:

$$e_V = u_V \int_{\tau=0}^t v_I \left[R \int_{t=\tau}^{\tau=t} (G_{(t)} dt)^n \right] d\tau \quad (10)$$

When there are many phases precipitating into the same nucleation sites of one type, each phase will have an extended volume given by Equation (10). The total extended volume for all phases since the onset of nucleation is:

$$e_{V(t)}^{\text{total}} = e_{V(t)}^A + e_{V(t)}^B + \dots + e_{V(t)}^N \quad (11)$$

Substituting the e_V value for each phase as given in Equation (10) into Equation (11) gives:

$$e_V^{\text{total}} = u_V \sum_{i=A}^N \int_{\tau=0}^t v_I \left[R \int_{t=\tau}^{\tau=t} (G_{(t)} dt)^n \right] d\tau \quad (12)$$

The extended volume is governed only by the kinetics of nucleation and crystal growth. The real volume is governed by the kinetics of nucleation and growth, by the effects of mutual interference of growing crystals, and by the covering up of nucleation sites by growing crystals.

If the relationship between the transformed volume (T_V) and the extended volume (e_V) is defined, then an equation can be written

relating the processes of nucleation, crystal growth, mutual interference of growing crystals, and the covering up of nucleation sites by growing crystals in terms of nucleation and crystal growth only. This relationship is found as follows.

Consider a small, random volume, V . A fraction of this volume remains without new crystals at time t . After a time interval dt , the real and extended volumes expand by $d^T V$ and $d^e V$ respectively. Next consider many expansive occurrences; on an average, a fraction $(1 - \frac{T_V}{u_V})$ (where T_V is the volume of new crystals) of $d^e V$ will lie in an untransformed region and thus contribute to $d^T V$. This allows $d^T V$ to be related to $d^e V$ as follows:

$$d^T V = (1 - \frac{T_V}{u_V}) d^e V \quad (13)$$

Upon integration, Equation (13) gives:

$$e_V = - u_V \ln (1 - \frac{T_V}{u_V}) \quad (14)$$

Substituting Equation (12) into Equation (14) gives:

$$- u_V \ln (1 - \frac{T_V}{u_V}) = u_V \sum_{i=A}^N \left(\int_{\tau=0}^t v I[R \int_{t=\tau}^t (G_{(t)} dt)^n] d\tau \right) \quad (15)$$

Dividing both sides by u_V and raising both sides to the exponential gives:

$$1 - \frac{T_V}{u_V} = \exp \left[- \sum_{i=A}^N \left(\int_{\tau=0}^t v I[R \int_{t=\tau}^t (G_{(t)} dt)^n] d\tau \right) \right] \quad (16)$$

u_V can be any volume of solid carbonates, packed carbonate particles, or carbonate particles and solution, etc. T_V is always the total solid volume of the transforming crystals.

It should be mentioned that in certain cases T_V will never reach u_V . This may occur for example, in dissolution-reprecipitation transformations of a volume of carbonate grains and water where only the volume of the grains is transformed. The result is the same as if a transformation had been quenched before completion.

Graphically, the result of a transformation where T_V will never equal u_V (or of a quenched transformation before u_V equals T_V) is a truncation of the sigmoidal time $\frac{T_V}{u_V}$ curve predicted by Equation (16) (see Figure 1).

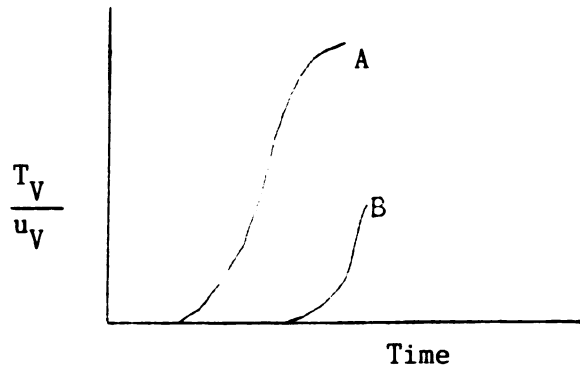


Figure 1: Reaction progress versus time curves
Curve A = reaction where T_V eventually reaches u_V . Curve B = reaction where T_V never reaches u_V .

Equation (16) is one of the general equations for the precipitation of carbonates within the thermodynamic stability field of dolomite when random nucleation per unit volume is occurring. Equation (16) allows for the precipitation of more than one phase. It takes into account mutual interference of growing crystals and the covering up of nucleation sites during growth. The equation can be arranged to model time-dependent heterogeneous nucleation and time-independent growth, and time-independent heterogeneous nucleation and time-dependent crystal

growth.

A. Time-dependent heterogeneous nucleation and time-independent growth

For this case Equation (16) becomes:

$$1 - \frac{T_V}{u_V} = \exp \left[- N_0 \sum_{i=A}^N \int_{\tau=0}^t J_i \exp^{\sum_{i=A}^N J_i \tau} [R \int_{t=\tau}^t (Gdt)^n] d\tau \right] \quad (17)$$

where N_0 is the number of nucleation sites of one type and J_i is the nucleation rate of phase i per site for one type of nucleation site.

The expression $N_0 J \exp^{\sum_{i=A}^N J_i t}$ is derived as follows (adapted from Avrami 1939). If there are N_0 sites per unit volume at $t=0$, then after a small time interval the number of sites that disappear is:

$$dN = - N \sum_{i=A}^N J dt \quad (18)$$

Integration of Equation (18) gives the number of sites remaining at any time t :

$$\int_{N=N_0}^N \frac{dN}{N} = - \int_0^t \sum_{i=A}^N J dt = \ln \frac{N}{N_0} = \sum_{i=A}^N J t \quad (19)$$

Taking the exponential of both sides and dividing both sides by N_0 gives:

$$N(t) = N_0 e^{\sum_{i=A}^N J t} \quad (20)$$

Equation (20) represents the number of nucleation sites left at any time. The rate at which these sites disappear is the time-dependent

nucleation rate per unit volume:

$$\frac{d^v N}{dt} = v_{N_0} \sum_{i=A}^N J \exp \sum_{i=A}^N Jt \quad (21)$$

Setting $t=\tau$ Equation (21) can be substituted into Equation (16) to give Equation (17). For $i=A$ and a constant crystal growth rate in three dimensions, Equation (17) reduces to Equation (20) of Avrami (1940).

If a nucleation induction period is to be considered, then using the expression $v_{It} = v_I \exp \frac{-k}{t}$ (Frenkel 1946, see also Kashchiev 1969), the disappearance of nucleation sites with time for one type of active site is given by:

$$dN = N \sum_{i=A}^N v_J \exp \frac{-k}{t} \quad (22)$$

Integrating by parts gives:

$$N(t) = N_0 \exp \left[\sum_{i=A}^N J \exp \frac{-k}{t} + \frac{k}{t} Ei \left(\frac{-k}{t} \right) \right] \quad (23)$$

where Ei denotes the integral exponential function and k is the time until steady state nucleation is attained.

The time-dependent rate of nucleation is the change in the number of nucleation sites with time:

$$\frac{d \left(N_0 \left[\exp \sum_{i=A}^N J \exp \frac{-k}{t} + \frac{k}{t} Ei \left(\frac{-k}{t} \right) \right] \right)}{dt} \quad (24)$$

Setting $t=\tau$, Equation (24) can be substituted into Equation (17) instead of Equation (21) when a nucleation induction period is to be considered.

B. Time-independent heterogeneous nucleation and time-dependent growth

$$1 - \frac{T_V}{u_V} = \exp - \sum_{i=A}^N \left(R^V I \int_{t=\tau}^t (Gdt)^n d\tau \right) \quad (25)$$

where $^V I$ is the time-independent heterogeneous nucleation rate per unit volume for one type of site.

The derivation of Equations (21) and (29) only applies (in a quantitative sense) to random nucleation of the volume-transforming carbonates throughout the volume being considered ($^u V$).

The general form of an equation when nuclei are confined to the surface of sedimentary particles and when the crystals from these surfaces can impinge upon the crystals from adjacent surfaces as well as impinge upon each other is:

$$1 - \frac{T_V}{u_V} = \exp (fn) \quad (26)$$

where (fn) is a function of nucleation and growth rate similar to those rates described previously. Simple examples of this function are derived in Cahn (1956). Derivations of other geologically meaningful examples of this function will not be presented here.

III THE VALIDITY OF THE DERIVED EQUATIONS AS COMPARED TO EXPERIMENTS

The purpose of this section is to examine experimental evidence which is supportive of the equations' applicability to carbonate precipitation.

Figure 2 represents the dissolution-reprecipitation transformation of calcite to dolomite via an intermediate high magnesium calcite.

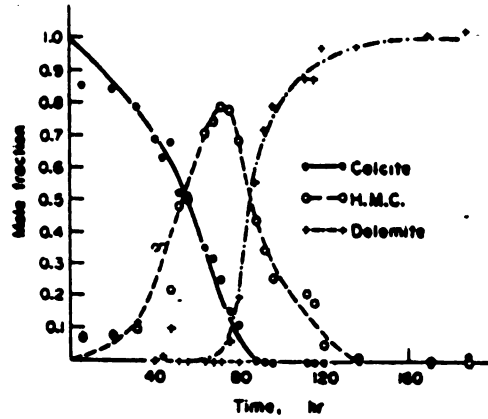


Figure 2: Calcite to dolomite transformation (from Katz and Matthews (1977)).

Curves B and C are sigmoidal in shape indicating that the fraction of material increases with time by an exponential function. The presence of these sigmoidal curves during the dissolution-reprecipitation transformation reactions in Figure 2 indicate that equations of the type given by (17), (25), and (26) are applicable. Figure 2 and Table 1 (see Appendix) indicate that metastable carbonate phases can precipitate abundantly within the thermodynamic stability field of dolomite.

The equations can account for the precipitation of metastable phases as follows. Under experimental conditions, nucleation occurs heterogeneously on a limited number of nucleation sites and therefore Equation (17) can be used to explain this. Assuming that each precipitating phase has a constant growth rate which is equal in three dimensions, Equation (17) becomes:

$$1 - \frac{T_V}{u_V} = \exp - N_0 \sum_{i=A}^N \frac{RG}{\tau} \int_{\tau=0}^t J_i \exp \left(- \sum_{j=A}^N \int_{\tau=0}^t J_j d\tau \right) (t-\tau) d\tau \quad (27)$$

This equation can then be integrated to give:

$$1 - \frac{T_V}{u_V} = \exp - N_0 \sum_{i=A}^N \frac{6R_i G_i}{\sum_{i=A}^N J} \left(\exp^{-\sum_{i=A}^N Jt} - 1 + \sum_{i=A}^N Jt - \frac{\sum_{i=A}^N J^2 t^2}{2} + \frac{\sum_{i=A}^N J^3 t^3}{6} \right) \quad (28)$$

Consider a solution supersaturated with respect to dolomite such that the solution is also supersaturated with respect to magnesium calcite and protodolomite. Let $X^c =$

$$\frac{6^c R}{\sum_{i=A}^N J} \left(\exp^{-\sum_{i=A}^N Jt} - 1 + \sum_{i=A}^N Jt - \frac{\sum_{i=A}^N J^2 t^2}{2} + \frac{\sum_{i=A}^N J^3 t^3}{6} \right)$$

where $\sum_{i=A}^N J_i$ is the summed nucleation rate of all precipitating phases for one type of nucleation site.

Similarly, let X^p and X^d represent protodolomite and dolomite respectively. Then substituting these values into Equation (28) gives:

$$1 - \frac{T_V}{u_V} = \exp - [N_0 ({}^c G' X^c + {}^p G' X^p + {}^d G' X^d)] \quad (29)$$

where ${}^c G'$, ${}^p G'$, and ${}^d G'$ are the growth rates for calcite, protodolomite and dolomite respectively.

If the product of growth rate and time-dependent nucleation rate of calcite (${}^c G' \times X^c$) is considerably greater than the products of time-dependent nucleation rate and growth rate of protodolomite (${}^p G' \times X^p$) and dolomite (${}^d G' \times X^d$), then (${}^p G' \times X^p$) and (${}^d G' \times X^d$) are negligible compared to (${}^c G' \times X^c$) and thus Equation (29) becomes:

$$1 - \frac{T_V}{u_V} = \exp^{-N_0^c G^c X^c} \quad (30)$$

If $(^c G^c \times X^c) = (^p G^p \times X^p) = (^d G^d \times X^d)$, then:

$$1 - \frac{T_V}{u_V} = \exp - [N_0 (^c G^c X^c + ^p G^p X^p + ^d G^d X^d)] \quad (31)$$

and the final transformed volume will contain equal amounts of dolomite, protodolomite and magnesium calcite.

All of the equations therefore can account for the precipitation of metastable phases when the nucleation and growth rates relative to other precipitating phases are significant.

In conclusion, supportive evidence for the equations in being able to predict the dissolution-reprecipitation transformation of carbonates is twofold. 1) The equations predict the sigmoidal-shaped curves for the dissolution-reprecipitation of carbonates. These curves are observed in experimental data (see Figure 2). 2) The equations can account for the precipitation of one or more metastable phases and predict that these phases should precipitate sigmoidally with time. This is also observed experimentally.

IV APPLICATION OF THE EQUATIONS TO EXPERIMENTAL AND NATURAL SITUATIONS

The purpose of this section is to qualitatively apply the equations to four aspects of the precipitation of carbonates within the thermodynamic stability field of dolomite. This will demonstrate how these equations may be used to explain experimental and natural situations.

A. Proposed explanation for sequences of metastable phases prior to the precipitation of the stable phases (Ostwald's steps)

In this study and in the study of Katz and Matthews (1977), a sequence of metastable phases have been observed during the dissolution-reprecipitation transformation of $4\text{MgCO}_3 \cdot \text{Mg}(\text{OH})_2 \cdot 4\text{H}_2\text{O}$, aragonite and calcite (see Appendix). The previously derived equations will provide an explanation for these observed sequences after the following five paragraphs are presented.

From the classical nucleation theory, a relationship for the nucleation rate per site type can be derived as follows. Under steady state conditions, the rate of nucleation onto a substrate is given by Turnbull and Fisher (1949):

$$Q = \frac{N_s}{h} \exp^{-\frac{G}{RT}} \exp^{-\frac{Bz}{R T} \frac{v}{(\ln \frac{s^*}{s})^2}} \quad (32)$$

where Q = the nucleation rate per second

N_s = the number of ions in a boundary layer on the substrate surface

R = the gas constant per ion or molecule

T = temperature

h = Planck's constant

G = Gibbs function of activation for diffusion

B = nucleus shape factor

z = total surface free energy of the nucleus

v = volume per molecule in the solid

$\frac{s^*}{s}$ = supersaturation ratio (saturation is the minimal saturation state necessary to form a nucleus on the substrate)

(Modified from Strickland-Constable 1968).

The nucleation rate per site for one type of site is given by:

$$J = \frac{Q}{\text{total number of sites}} \quad (33)$$

Equation (33) can be simplified as follows. Noting that the term

$\frac{N_s RT}{h} \exp \frac{-G}{RT}$ is essentially constant at constant temperature, then for a certain substrate it can be set equal to K. Doing this gives:

$$J = K \exp - \frac{Bz v}{R T (\ln \frac{s^*}{s})} \quad (34)$$

Equation (34) can be used to construct a plot of saturation state versus the nucleation rate per site type for dolomite and each metastable phase. Unfortunately, the plot (see Figure 3) must be constructed with relative values since values for z of carbonate phases for heterogenous nucleation are not available. Discussions using Figure 3 therefore can only be in relative or qualitative terms.

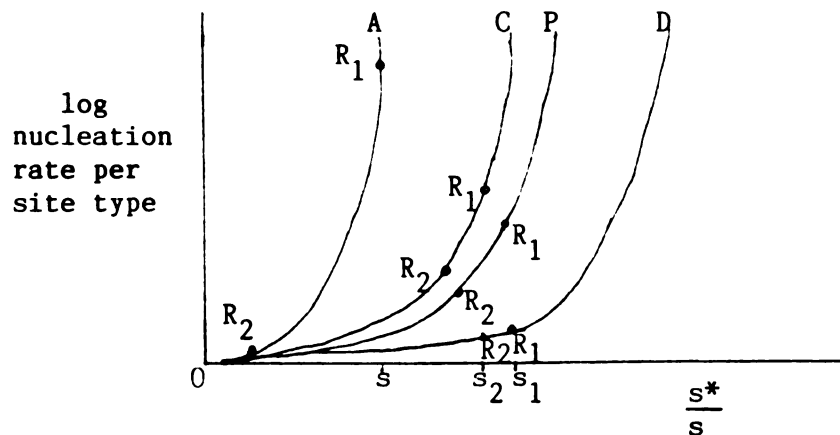


Figure 3: Nucleation rate per site versus supersaturation

Note: $\frac{s^*}{s}$ is not fixed but depends on the curve being viewed. For example, when viewing the dolomite curve, $\frac{s^*}{s}$ represents the dolomite supersaturation ratio. Curves are constructed such that $Bz v$ of $A < Bz v$ of $C < Bz v$ of $P < Bz v$ of D . Curve D is the thermodynamically stable phase. A, C, P, D are metastable carbonate phases composed of some combination of $\text{Ca} + \text{CO}_2$, $\text{Mg} + \text{CO}_2$, or $\text{Ca} + \text{Mg} + \text{CO}_2$. s , s_1 , s_2 , x , y are explained in the text.

Figure 3 illustrates that the nucleation rate of a metastable phase can increase much faster than the nucleation rate of the

thermodynamically stable phase with an increase in the saturation state of the stable phase when the following two conditions are met. First, the starting saturation ratio $\frac{s^*}{s}$ in terms of the saturation state of the stable phase must be appropriate (i.e. it must occur before the exponential upsweep of the stable phase curve). Second, an increase in the saturation state of the stable phase must provide an appropriate increase in the saturation state of the metastable phase. For example, consider metastable phase A represented by curve A (see Figure 3). It has the appropriate starting saturation ratio (given as s on curve D and O on curve A) and has the product $Bz'v'$ appropriately lower than that product for curve D. When the saturation state of phase D is raised by the amount X for the stable phase D, producing an increase in Y of the saturation state for the metastable phase A, the nucleation rate of phase A increases by several orders of magnitude over the stable phase.

From this theoretically derived concept, the Ostwald's steps obtained during the transformation of $4MgCO_3 \cdot Mg(OH)_2 \cdot 4H_2O$, aragonite and calcite to dolomite in this study (see Table 1, Appendix) can be explained as follows.

Consider a substrate ($4MgCO_3 \cdot Mg(OH)_2 \cdot 4H_2O$) in contact with a dolomite supersaturated solution in a closed system. On this substrate there exists a number of nucleation sites of one type. Let a nucleus of aragonite have a nucleation rate versus the saturation state on these nucleation sites be represented by line A in Figure 3. Let the nucleation rate versus supersaturation of calcite, protodolomite and dolomite be represented by lines C, P, and D respectively in Figure 3.

If the solution in contact with the substrate has a dolomite supersaturation state of s_1 (which has a corresponding nucleation rate

R_1 for all phases indicated in Figure 3), then the nucleation rate of aragonite will be several orders of magnitude greater than all the other phases and recalling Equation (28) gives:

$$1 - \frac{T_V}{u_V} = \exp - [N_o^A G^A X^A] \quad (35)$$

If the growth rate of aragonite is competitive with the growth rate of the other phases, then the transformation will proceed to all or virtually all aragonite.

In a closed system, the transformation to aragonite has lowered the saturation state of dolomite within that system (see Interpretation of Results section in Appendix for reasoning). This lower dolomite saturation state coupled with the new aragonite surface provides a range of ΔG s of nucleation for all phases which are some combination of Ca^{2+} , Mg^{2+} , CO_3^{2-} .

If the nucleation and growth rates of certain metastable phases are much faster than the nucleation and growth rates for the thermodynamically stable phase, then this transformation will also convert to a metastable phase or phases in a manner exactly as explained previously for the transformation to aragonite. For example, a drop in the dolomite saturation state from s_1 to s_2 (see Figure 3) lowers the relative rate of nucleation of aragonite relative to protodolomite, low magnesium calcite and dolomite. If the rates of nucleation of protodolomite and low magnesium calcite are still much greater than the rate of nucleation of dolomite (a drop from R_1 to R_2 in Figure 3), then the aragonite will be transformed into these two phases instead of dolomite.

This process may be repeated several times before the precipitation of the thermodynamically stable phase thus giving rise to the

the sequences illustrated in Table 1 (see Appendix). The basic concepts used here may explain sequences of metastable phases (Ostwald's step rule) in other systems as well.

B. Proposed explanation for the distribution of carbonates from marine-type waters

The most notable features of Table 2 are the virtual absence of the thermodynamically stable phase, dolomite and the widespread precipitation of various types of metastable carbonate phases. Equilibrium thermodynamics does not provide an easily attainable explanation for this distribution and thus a kinetic explanation must be sought.

Using the explanation of Ostwald's steps given in the previous section, the distribution of carbonates in Table 2 can be explained by the equations in the following manner. The nucleation and/or growth rates of aragonite and magnesium calcite are substantially faster than the rates of nucleation and/or growth of protodolomite in shallow marine solutions supersaturated with respect to aragonite and high magnesium calcite. This allows these phases to transform pore space into aragonite and magnesium calcite preferentially over protodolomite during the time the pores are bathed in this solution. This is equivalent to the situation where $c_{G'X'} = A_{G'X'} \gg P_{G'X'}$ and then substituting these values into Equation (29).

Not until a marine solution has a lower rate of precipitation of aragonite and magnesium calcite will protodolomite and/or possibly low magnesium calcite be able to precipitate (or transform the substrate if the solution is undersaturated with respect to aragonite and magnesium calcite) during the time these substrates are in contact with that solution.

Table 2: DISTRIBUTION OF MARINE CARBONATES

Environment	Carbonate Minerals Precipitated	Saturation State	Substrate Type	References
shallow normal marine *****	aragonite magnesium calcite *****	> aragonite *****	aragonite magnesium calcite *****	Berner 1971 Bathurst 1975 *****
deep normal marine *****	ordered dolomite protodolomite low magnesium calcite *****	(proposed) < aragonite *****	aragonite magnesium calcite coccoliths *****	Saller 1984 Mullins et al. 1985 *****
marine sulfate reduction *****	protodolomite some ordered dolomite *****	< low magnesium calcite *****	low magnesium calcite *****	Baker and Burns 1985 *****
sabka Abu Dhabi *****	protodolomite some ordered dolomite with depth low magnesium calcite *****	< aragonite *****	aragonite *****	McKenzie 1981 Kinsman 1964 *****

There are two principal ways in which the product (growth rate \times nucleation rate) for aragonite and high magnesium calcite can be lowered relative to this product for protodolomite and/or low magnesium calcite. First, a change in the dolomite saturation state such that the activity of Ca^{2+} and/or CO_3^{2-} is lowered. This can reduce (as suggested in the previous section) the rates of nucleation of these two phases by an amount greater than it reduces the rate of nucleation of protodolomite.

Second, the addition or removal of nucleation and/or growth inhibiting substances which may inhibit the nucleation and/or growth rate of one carbonate phase more than another may also lower the product of growth rate \times nucleation rate. There is some evidence suggesting inhibition of carbonate precipitation in marine-type waters (Baker and Kastner 1981, Berner et al. 1978, Chave and Seuss 1967, Seuss 1970), but whether there are any selective inhibitors remains to be demonstrated.

The placement of ordered dolomite within this scheme is not as simple because there is not definite evidence which suggests that ordered dolomite is able to nucleate onto aragonite or magnesium calcite substrates at the dolomite saturation states found in seawater or in modified seawater. There are therefore, two possible reasons for the present distribution of ordered dolomite in marine-type waters. First, ordered dolomite is outcompeted by faster nucleating and growing metastable phases on aragonitic, calcitic, and protodolomitic substrates except when the dolomite saturation state is such that it is close to or below protodolomite saturation. The potentially low dolomite saturation state will thus produce low nucleation and growth rates of dolomite. These rates may be slow even in terms of geologic time thereby preventing dolomite from precipitating to any large extent

during the time a substrate is in contact with such a solution. Second, the surface free energy to form a dolomite is so much higher on aragonite and magnesium calcite substrates that its nucleation rate on those substrates is zero at the dolomite saturation state in marine-type waters. It would therefore only be able to nucleate on a specific substrate such as a protodolomite.

C. Proposed explanation for the effect of substrate grain size on the transformation rate

If the number of initial nucleation sites on a substrate are directly proportional to the surface area, then a fine grained sediment will have a greater surface area per unit volume and thus a greater number of nucleation sites per unit volume than a coarse grained sediment.

The greater number of initial nucleation sites per unit volume in the fine grained sediment with respect to the coarse grained sediment results in a larger number of nuclei per unit volume in the fine grained sediment compared to the coarse grained sediment. Examination of Equation (17) indicates that at any time t , the larger the value of the combined N_0 , the closer $1 - \frac{T}{u_v}$ is to zero or the closer the transformation is to completion (see Figure 4). Thus a fine grained sediment can undergo transformation at a faster rate than a coarse grained sediment.

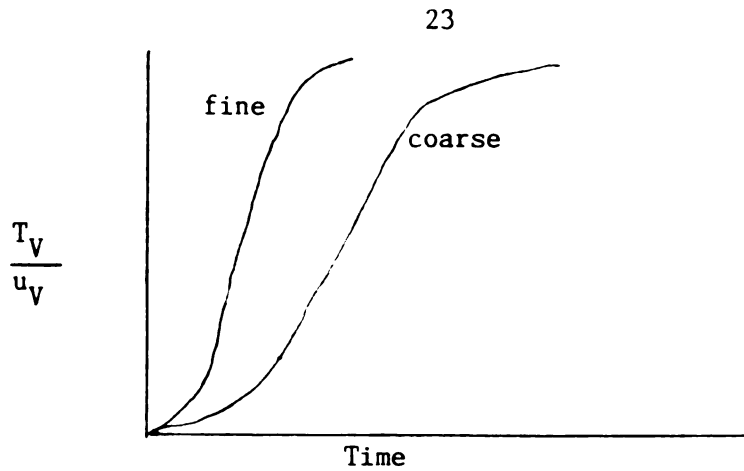


Figure 4: Proposed curves for coarse and fine material

Bartlett (1984) experimentally examined the effect of carbonate substrate size on the rate of transformation of that substrate to dolomite. His results point out the importance of the number of nucleation sites per unit volume on the transformation rate of carbonate sediments to dolomite. His curves differ somewhat from those in Figure 4. The reason for this discrepancy may be that other factors besides the number of nucleation sites per unit volume were important during his transformation reactions. It is not within the scope of this study to discuss potential candidates for these factors.

D. Proposed equation describing the porosity and permeability of dolomitic rocks

Equations describing the generation of porosity and permeability in carbonate sediments as a function of time do not exist. The porosity and permeability of dolomitic rocks are dependent on the density per unit volume of dolomite crystals and the degree of mutual interference between these crystals. Therefore, porosity and permeability can be explained quantitatively in terms of the equations proposed in this study.

For example, consider a volume of carbonate sediments being

transformed into a dolomitic rock. If the untransformed portion of the carbonate is considered to be porosity (it gets removed through later diagenesis), then the porosity of the dolomitic rock will be equal to $\frac{T_V}{u_V}$. From Equation (17):

$$\frac{T_V}{u_V} = 1 - \exp \left[- N_0 \sum_{i=A}^N \left(\int_{\tau=0}^t J \exp^{-J\tau} \left[R \int_{t=\tau}^t (Gd\tau)^n d\tau \right) \right] \right] \quad (36)$$

Permeability will depend on porosity and the degree of mutual interference between dolomite crystals and therefore will vary directly with Equation (36):

$$\text{permeability} = \text{fcn} \frac{T_V}{u_V} \quad (37)$$

V CONCLUSION

Equations have been derived for the precipitation of carbonate phases within the thermodynamic stability field of dolomite in terms of the two kinetic processes: nucleation and crystal growth. The equations can be used quantitatively and qualitatively in natural and experimental cases where transformation of a phase proceeds by random nucleation within that volume.

The equations are not restricted to carbonate precipitation but can be applied to the transformation of a volume by precipitation of one or more phases in igneous and metamorphic as well as sedimentary environments if the following condition is met. In the case to be considered all precipitating phases can nucleate on all available nucleation sites.

APPENDIX

APPENDIX

A. Experimental procedure

The purpose of these experiments was to transform various carbonate substrates to dolomite. Particular attention was given to the solubility of that substrate relative to the other substrates and the sequence of metastable carbonate phases precipitating prior to the precipitation of dolomite.

All experiments were performed inside 10 ml stainless steel bombs and Parr model #4749 Teflon-lined bombs with a 23 ml capacity.

Temperature was kept at 210°C for all experiments inside an automatic temperature-controlled Linberg oven.

The reaction solutions were prepared by dissolving analytical grade $\text{CaCl}_2 \cdot 2\text{H}_2\text{O}$ (Fischer) and $\text{MgCl}_2 \cdot 6\text{H}_2\text{O}$ (Mallinckrodt) into twice-distilled water in separate erlenmeyer flasks to a concentration of 1M.

The reactants used were $4\text{MgCO}_3 \cdot \text{Mg}(\text{OH})_2 \cdot 4\text{H}_2\text{O}$, reagent grade calcite and ground natural aragonite.

Experimental charges consisted of .2000 grams of a reactant, 5.4 ml of CaCl_2 , and 3.6 ml of MgCl_2 , (only one mineral per charge at any one time). Charges were allowed to react for a certain length of time and then quenched with cold water. The contents of each charge were emptied into Whatman #1 11 cm filter paper and then rinsed with distilled water. The charge contents and filter paper were then dried together at 180°C until thoroughly dry. The charge contents were then placed in a small plastic container with a snap-on cap. The container was then marked with the type of reactant and the length of time elapsed between placing the charge into the oven and the quenching of that charge.

Phase identification of the solid charge contents was made by

X-ray powder diffraction using Ni filtered CuK radiation. Scanning was done from 14°C to 43° C 2θ at a rate of .5°/minute. Samples were scanned as a powder smear on a recessed portion of a glass slide. The internal standard used was fluorite.

B. Results

See Table 1: Experimental Results from X-ray Diffraction

C. Interpretation of Results

By extrapolating Rosenberg's et al. (1967) experimental boundaries for the stability field of dolomite in chloride solutions to 210°C, the solutions within the charges are found to lie within the thermodynamic stability field of dolomite.

Table 1 indicates that dolomite, regardless of the initial reactant, precipitates after the precipitation of a series of one or more metastable phases. Based on Katz and Matthews (1977) work it is assumed that one metastable phase replaces another through dissolution-reprecipitation in these experiments.

The dissolution-reprecipitation sequence is interpreted to represent a decreasing dolomite saturation state within the charge as time progresses. The following explanation is given in support of this. For one phase to undergo replacement of another phase through a dissolution-reprecipitation transformation, that phase must be able to dissolve. Consider the series of observed phases when aragonite was used as the initial reactant:

1) At $t=0$, the charge is saturated with aragonite

2) As protodolomite precipitates, the product of $a_{Ca^{2+}} \times a_{CO_3^{2-}}$ must decrease in order for aragonite to dissolve and eventually be

Table 1: EXPERIMENTAL RESULTS FROM X-RAY DIFFRACTION

Solid Reactant at t=0	Time (hrs)	Solid Products	Relative Heights of Main Peaks	Sample #
4MgCO ₃ ·Mg(OH)·4H ₂ O	1/2	C 11 mole% Mg A	A/C = 3.6	25B
"	1/2	C 11 mole% Mg A	A/C = 2.6	24B
"	3/4	C 11 mole% Mg P 44 mole% Mg A	A/C = .85 A/P = .30	20B
"	3/4	C 11 mole% Mg P 44 mole% Mg A	A/C = .8 A/P = 2	21B
"	1	C 11 mole% Mg P	A/C = .5 A/P = .6	18B
"	1	C 11 mole% Mg P 44 mole% Mg A	A/C = 1.4 A/P = 1.0	16B
"	1	C 11 mole% Mg P 44 mole% Mg A	A/C = .4 A/P = .5	19B
"	1 hr 10 min	C 11 mole% Mg P 44 mole% Mg A	A/C = .8 A/P = .5	22B
"	1 hr 10 min	C 11 mole% Mg P 44 mole% Mg A	A/C = 1.2 A/P = 1.0	23B
"	1 1/2	C 11 mole% Mg P 46 mole% Mg	P/C = 3.8	14B

Table 1 (cont'd.)

Solid Reactant at t=0	Time (hrs)	Solid Products	Relative Heights of Main Peaks	Sample #
4MgCO ₃ ·Mg(OH)·4H ₂ O	1 1/2	C 11 mole% Mg P 46 mole% Mg	P/C = 1.5	13B
"	"	"	"	"
"	1 1/2	C 11 mole% Mg P 46 mole% Mg	P/C = 2.2	12B
"	"	"	"	"
"	2	C 11 mole% Mg P 46 mole% Mg	P/C = 4.8	9B
"	"	"	"	"
"	2	C 11 mole% Mg P 46 mole% Mg	P/C = 3.4	10B
"	"	"	"	"
"	2	C 11 mole% Mg P 46 mole% Mg	P/C = 3.4	11B
"	"	"	"	"
"	3	C 11 mole% Mg P 46 mole% Mg	P/C = 5.6	6B
"	"	"	"	"
"	3	C 11 mole% Mg P 46 mole% Mg	P/C = 5	5B
"	"	"	"	"
"	4	P 47 mole% Mg	"	4B
"	"	"	"	"
"	4	P 47 mole% Mg	"	3B
"	"	"	"	"
"	4	P 47 mole% Mg	"	2B
"	"	"	"	"
"	4	P 47 mole% Mg	"	1B
"	"	"	"	"
"	6	P 48 mole% Mg	"	26B
"	"	"	"	"
"	7 3/4	D 49 mole% Mg ordering peaks	"	27B
"	"	"	"	"
Aragonite	2	C 12 mole% Mg P 43 mole% Mg	P/A = 2.4 C/A = 1.6	5C

Table 1 (cont'd)

<u>Solid Reactant at t=0</u>	<u>Time (hrs)</u>	<u>Solid Products</u>	<u>Relative Heights of Main Peaks</u>	<u>Sample #</u>
Calcite	24	P 41 mole% Mg minor H ? C	P/C = .05	11A
"	24	P 41 mole% Mg H ? C	P/C = .04 P/H = 1.0	10A
"	24	P 41 mole% Mg minor H ? C	P/C = .08	9A
"	24	P 41 mole% Mg C	P/C = .1	8A
"	25	P 41 mole% Mg C	P/C = 1.0	18A
"	25 1/2	P 41 mole% Mg C	P/C = .18	17A
"	26 1/2	P 41 mole% Mg C	P/C = .26	19A
"	26 1/2	P 41 mole% Mg C	P/C = .30	20A
"	29	P 41 mole% Mg	P/C = .17	24A
"	29	P 41 mole% Mg C	P/C = 1.22	23A
"	28	P 41 mole% Mg C	P/C = .22	29A

Table 1 (cont'd.)

Solid Reactant at t=0	Time (hrs)	Solid Products	Relative Heights of Main Peaks	Sample #
Aragonite	3	C 12 mole% Mg P 43 mole% Mg	P/C = 1.5	1C
"	3	C 12 mole% Mg P 43 mole% Mg	P/C = 1.1	2C
"	4	C 12 mole% Mg P 44 mole% Mg	P/C = 1.2	4C
"	4	C 12 mole% Mg P 44 mole% Mg	P/C = 1.7	7C
"	5	P 47 mole% Mg		5C
"	6	minor C P 47 mole% Mg		9C
"	6	minor C P 47 mole% Mg		8C
"	18	D 49 mole% Mg ordering peaks		11C
"	18	D 49 mole% Mg ordering peaks		10C
"	23 1/2	D 49 mole% Mg ordering peaks		13C
Calcite	23	H ? C		15A
"	23	P 41 mole% Mg H ? C	P/C = .09	13A

Table 1 (cont'd.)

Solid Reactant at t=0	Time (hrs)	Solid Products	Relative Heights of Main Peaks	Sample #
Calcite	29	P 41 mole% Mg C	P/C = 1.52	22A
"	53	D 49 mole% Mg ordering peaks		25A
"	8 days 4 hrs	D 49+ mole% Mg ordering peaks		20A
* 4MgCO ₃ ·Mg(OH) ₂ ·4H ₂ O	1	C 11 mole% Mg minor P A	A/C = 3.25	1G
* "	"	C 11 mole% Mg P 44 mole% Mg minor A	P/C = 3.0	2G
* "	"	P 49 mole% Mg		3G
* "	"	D 49 mole% Mg ordering peaks		4G
* Aragonite	4	C 11 mole% Mg P 44 mole% Mg	P/C = 2	1H
*	8	P 47 mole% Mg C 11 mole% Mg		2H
* Calcite	30	P 40 mole% Mg C	P/C = 1	1I
*	44	P 40 mole% Mg D 49 mole% Mg	D/P = 3	2I

A = Aragonite, C = Calcite, D = Dolomite, H = Huntite, P = Protodolomite
 * = Teflon-lined bombs were used

replaced. This occurs because the ΔG of dissolution of aragonite is positive at aragonite supersaturation, zero at aragonite saturation and negative at aragonite undersaturation. Thus the energy input and direction of flow necessary to drive the kinetic processes of dissolution on the aragonite surface can occur only at aragonite undersaturation. Therefore the $a\text{Ca}^{2+} \times a\text{Mg}^{2+} \times a\text{CO}_3^{2-}$ is lower after protodolomite precipitates than at $t=0$.

3) As dolomite replaces protodolomite, the $a\text{Ca}^{2+} \times a\text{Mg}^{2+} \times a\text{CO}_3^{2-}$ must be lower than step 2 above. Thus there is a general decrease in the dolomite saturation state with time.

A theoretical explanation for the observed sequences of metastable phases precipitating prior to dolomite precipitation is given in section IV of this paper.

REFERENCES

REFERENCES

- Avrami, M., 1939, Kinetics of phase change, I. General Theory. Jour. Chem. Physics, 7: 1103-1112.
- _____, 1940, Kinetics of phase change, II. Transformation-time relations for random distribution of nuclei. Jour. Chem. Physics, 8: 212-224.
- _____, 1941, Kinetics of phase change, III. Granulation, phase change and microstructure. Jour. Chem. Physics, 9: 177-184.
- Baker, P.A. and Burns, S.J., 1985, Occurrence and formation of dolomite in organic-rich continental margin sediments. Amer. Assoc. Petroleum Geol. Bull. 69: 1917-1930.
- Baker, P.A. and Kastner, M., 1981, Constraints on the formation of sedimentary dolomite. Science, 213: 214-216.
- Bartlett, T.R., 1984, Synthetic dolomitization: rate effects of variable mineralogy, surface area, external CO_2 and crystal seeding. M.S. Thesis, Michigan State Univ.
- Bathurst, R.G.C., 1975, Carbonate sediments and their diagenesis, 2nd Ed., Elsevier, Amsterdam, The Netherlands, 658 p.
- Berner, R.A., 1971, Principles of chemical sedimentology, McGraw-Hill Book Co., New York, 240 p.
- Berner, R.A., Westrich, J.T., Graber, R., Smith, J. and Martens, C.S., 1978, Inhibition of aragonite precipitation from supersaturated seawater: a laboratory and field study. Am. Jour. Sci., 278: 816-837.
- Cahn, J.W., 1956, The kinetics of grain boundary nucleated reactions. Acta Metall., 4: 449-459.
- Chave, K.E. and Suess, E., 1967, Suspended minerals in seawater. Trans. N.Y. Acad. Sci., Ser. II, 29: 991-1000.
- Fairbridge, R.W., 1957, The dolomite question. In: R.J. LeBlanc and J.G. Breeding (eds.), Regional aspects of carbonate deposition. Soc. Econ. Paleontologists and Mineralogists, Spec. Pub. 5: 125-178.
- Frenkel, J.I., 1946, Kinetic theory of liquids. Oxford Univ. Press, Oxford.

- Friedman, G.M. and Sanders, J.E., 1967, Origin and occurrence of dolostones. In: G.V. Chilingar, H.J. Bissell and R.W. Fairbridge (eds.), Carbonate rocks, Part A: origin occurrence and classification. Elsevier, Amsterdam, The Netherlands, p. 267-348.
- Gaines, A.M., 1980, Dolomitization kinetics: recent experimental studies. In: D.H. Zenger, J.B. Dunham and R.L. Ethington (eds.), Concepts and models of dolomitization. SEPM Spec. Publ. 28: 81-86.
- Ingerson, E., 1962, Problems of the geochemistry of sedimentary carbonate rocks. *Geochim. et Cosmochim. Acta*. 26: 815-847.
- Johnson, W.A. and Mehl, R.F., 1939, Reaction kinetics in processes of nucleation and growth. *Amer. Inst. Mining Eng. Publ.* 1089: 1-27.
- Kashchiev, D., 1969, Solution of the nonsteady state problem in nucleation kinetics. *Surface Sci.* 14: 209-220.
- Katz, A. and Matthews, A., 1977, The dolomitization of CaCO_3 : an experimental study at 252-295°C. *Geochim. et Cosmochim. Acta*. 41: 291-308.
- Kinsman, D.J.J., 1964, Recent carbonate sedimentation near Abu Dhabi, Trucial Coast, Persian Gulf. unpubl. Ph.D. diss., Imperial Coll., Sci. Tech., London.
- McKenzie, J.A., 1981, Holocene dolomitization of calcium carbonate sediments from the coastal sabkhas of Abu Dhabi, U.A.E.: a stable isotope study. *Jour. Geol.* 89: 185-198.
- Morrow, D.W., 1982a, Diagenesis 1. Dolomite-Part 1: The chemistry of dolomitization and dolomite precipitation. *Geoscience Canada*. 9: 5-13.
- _____, 1982b, Diagenesis 2. Dolomite-Part 2: Dolomitization models and ancient dolostones. *Geoscience Canada* 9: 95-107.
- Mullins, H.T., Wise, S.W., Jr., Land, L.S., Siegel, D.I., Masters, P.M., Hinchey, E.J. and Price, K.R., 1985, Authigenic dolomite in Bahamian periplatform slope sediment. *Geol.*, 13: 292-295.
- Rosenberg, P.E., Burt, D.M. and Holland, H.D., 1967, Calcite-dolomite-magnesite stability reactions in solutions: the effect of ion strength. *Geochim. et Cosmochim. Acta*. 31: 391-396.
- Saller, A.H., 1984, Petrologic and geochemical constraints on the origin of subsurface dolomite, Enewetak Atoll: an example of dolomitization by normal seawater. *Geol.*, 12: 217-220.
- Strickland-Constable, R.F., 1968, Kinetics and mechanisms of crystallization. Academic Press, London.
- Turnbull, D. and Fisher, J.C., 1949, Rates of nucleation in condensed systems. *Jour. Chem. Physics*. 17: 71-73.

- Suess, E., 1970, Interaction of organic compounds with calcium carbonate. I. Association phenomena and geochemical implications. *Geochim. Cosmochim. Acta*. 34: 157-168.
- Zenger, D.H., 1972, Dolomitization and uniformitarianism. *Jour. Geol. Education*. 20: 107-124.
- Zenger, D.H. and Dunham. J.B., 1980, Concepts and models of dolomitization-an introduction. In: D.H. Zenger, J.B. Dunham and R.L. Ethington (eds.). Concepts and models of dolomitization. *SEPM Spec. Publ.* 28: 1-9.

MICHIGAN STATE UNIV. LIBRARIES



31293007014008